In situ measurements of optical parameters in Lake Baikal with the help of a Neutrino telescope

Vasilij Balkanov, Igor Belolaptikov, Leonid Bezrukov, Aleksander Chensky, Nikolaij Budnev, Igor Danilchenko, Zhan-Arys Dzhilkibaev, Grigorij Domogatsky, Aleksander Doroshenko, Stanislav Fialkovsky, Oleg Gaponenko, Anatolij Garus, Tatiana Gress, Albrecht Karle, Arkadij Klabukov, Anatolij Klimov, Sergeij Klimushin, Andreij Koshechkin, Viktor Kulepov, Leonid Kuzmichev, Bajarto Lubsandorzhiev, Sergeij Lovzov, Thomas Mikolajski, Michail Milenin, Rashid Mirgazov, Andreij Moroz, Nikolaij Moseiko, Semen Nikiforov, Eleonora Osipova, Dirk Pandel, Andreij Panfilov, Yurij Parfenov, Anatolij Pavlov, Dmitrij Petukhov, Pavel Pokhil, Peter Pokolev, Elena Popova, Michail Rozanov, Valerij Rubzov, Igor Sokalski, Christian Spiering, Ole Streicher, Boris Tarashansky, Thorsten Thon, Ralf Wischnewski, and Ivan Yashin

We present results of an experiment performed in Lake Baikal at a depth of ~1 km. The photomultipliers of an underwater neutrino telescope under construction at this site were illuminated by a distant laser. The experiment not only provided a useful cross-check of the time calibration of the detector but also allowed us to determine inherent optical parameters of the water in a way that was complementary to standard methods. In 1997 we measured an absorption length of 22 m and an asymptotic attenuation length of 18 m. The effective scattering length was measured as 480 m. By use of $\langle \cos\theta \rangle = 0.95$ (0.90) for the average scattering angle, this length corresponds to a geometric scattering length of 24 (48) m.

OCIS codes: 010.3310, 010.4450, 010.7340, 290.5820, 290.5870.

1. Introduction

Propagation of light in optical media is governed by two basic phenomena: absorption and scattering. In the first case the photon is lost; in the second case it changes its direction. The inherent parameters generally chosen as a measure for these phenomena are the absorption length λ_{abs}, the scattering length λ_{sct}, and the scattering function (or scattering tensor if polarization is taken into account) $\beta(\theta)$.

Determining optical parameters for the water of deep lakes or oceans has considerable problems. Typical values for λ_{abs} in the window of maximum transparency are ~20 m for the clearest water in deep lakes[1,2] and 50 m for deep oceans.[3–5] Another important property of natural water is the strongly forward peaked scattering with $\langle \cos\theta \rangle = 0.85–0.96$ in oceans[6] or lakes[2,7] and scattering lengths of 10–50 m. Because of the long absorption and scattering lengths and the steep scattering function, devices for measuring these optical parameters in clear water have to be extremely precise and well calibrated.

In vitro measurements suffer from the comparatively short base length of the laboratory devices and from the fact that the samples of the medium can deteriorate before being analyzed in the laboratory. Furthermore for *in vitro* measurements it is rather difficult to perform long-term experiments and to observe seasonal variations of the optical parameters. *In situ* devices are difficult to handle, particularly for greater depths. On the other hand, only *in situ* measurements allow long-term observations of the medium, including implications of temporarily changing mechanical, chemical, biological, and thermal conditions.

In the course of preparing a deep-underwater neutrino telescope in Lake Baikal (see Section 2), *in situ* optical measurements have been carried out over several years. We have constructed a special device (see Refs. 1 and 8) and developed proper methods[2,7] to determine and to monitor the hydro-optical parame-

The authors' affiliations are listed in Appendix A.
Received 1 April 1999; revised manuscript received 26 July 1999.
0003-6935/99/336818-08$15.00/0

ters of the water body at the site of the Baikal Neutrino Telescope. The data from these measurements do not yield only the necessary input parameters for operation of the telescope but are interesting as well for environmental science.

In this paper we present results of optical measurements obtained in a way that is complementary to standard limnological (oceanological) methods by use of a laser as a light source and an underwater neutrino telescope as a light detector. This kind of telescope represents a new class of giant instrument that is now in operation at various locations in deep oceans and lakes[9] and even in glaciers. Being permanently operational over several years, underwater telescopes can perform, as a by-product and for calibration purposes, measurements of optical parameters as well as of water currents and bioluminescence.

We have measured the spatial and the temporal distribution of monochromatic light from a pulsed isotropic, pointlike source. From an analysis of the spatial distribution, we derive values for absorption length λ_{abs} and for the asymptotic attenuation length λ_{asm}. From the time delay of the short light flashes that arrive at the photomultipliers of the telescope, we derive λ_{eff}, which is an effective parameter describing scattering.

We describe the Baikal Neutrino Telescope in Section 2 and laser experiments to determine the optical parameters of the water in Section 3. In Section 4 we derive expressions for the light field as a function of the distance to an isotropic source. The experimental data are analyzed in Section 5, and values for parameters characterizing absorption and scattering are derived. Section 6 is the conclusion.

2. Baikal Neutrino Telescope

The Baikal Neutrino Telescope[10] exploits the deep water of a Siberian lake as a detection medium for secondary charged particles, such as muons or electrons, generated in neutrino interactions. Neutrinos are etheric particles characterized by their extremely rare interaction with all kinds of matter. They are supposed to be generated in cosmic particle accelerators such as the nuclei of active galaxies or binary star systems. Shielded by kilometers of water burden, underwater telescopes aim to detect the rare reactions of neutrinos from these exotic sources.

A lattice of photomultiplier tubes (PMT's) spread over a large volume records the Cerenkov light emitted by the relativistic charged particles. The light arrival times at the locations of the PMT's are measured to an accuracy of a few nanoseconds. From the time pattern the particle trajectory can be reconstructed with a resolution of 1–2 deg. In addition to the arrival times, the amplitudes of the signals are recorded. Typical amplitudes for particles triggering the array are in the few-photoelectron range.

The Neutrino Telescope NT-200 is being deployed at the southern part of Lake Baikal (Fig. 1). The distance to shore is 3.6 km, and the depth of the lake is 1366 m at this location. Figure 2 shows the instrumentation of the site. Strings anchored by

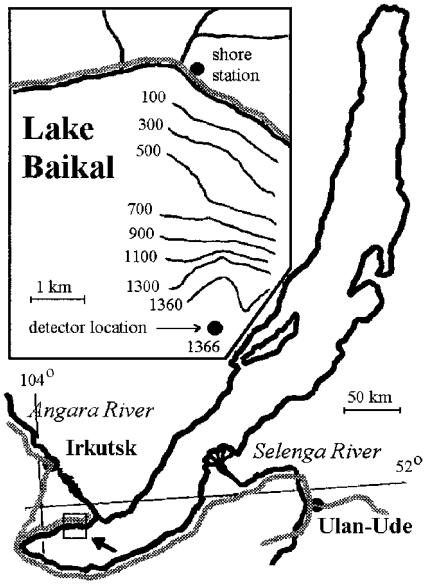

Fig. 1. Location of the Baikal experiment.

weights at the bottom are held in vertical position by buoys at various depths. The deployment of the detector elements is carried out in late winter when the lake is covered by a thick layer of ice. Three cables (1, 2, 3 in Fig. 2) connect the detector with the shore station. Each shore cable ends at the top of a string (4, 5, 6, respectively). String 7 carries the telescope. A special hydrometric string, 8, is equipped with instruments to measure the optical parameters of the water as well as water currents, temperature, pressure, and sound velocity. The spatial coordinates of the components of the telescope are monitored by an ultrasonic system consisting of transceivers 9–14 and receivers along the strings. The relative coordinates

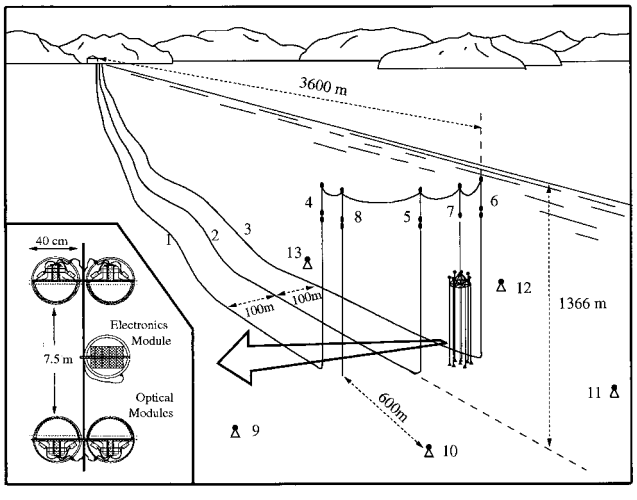

Fig. 2. Overall view of the NT-200 complex: 1–3, cables to shore; 4–6, string stations for shore cables; 7, string with the telescope; 8, hydrometric string; 9–14, ultrasonic emitters. The detail at bottom left, which hides ultrasonic emitter 14, shows two pairs of OM's together with the electronics module controlling the OM's. Shown are two pairs directed face to face.

of the components are determined with an accuracy of ~20 cm.

The telescope, NT-200, consists of eight substrings arranged at the center and the edges of an equilateral heptagon. The light detection elements are optical modules (OM's) containing a hybrid phototube, Quasar-370, with a hemispherical photocathode 370 mm in diameter.

The time resolution of the Quasar-370 is 3 ns for a single-photoelectron signal and improves to ~1 ns for large amplitudes. The OM's are arranged pairwise with the two phototubes operated in coincidence (see Fig. 2). If an event triggers at least three pairs within 500 ns, the light arrival time and the amplitude of each hit pair (channel) are recorded. Each of the eight strings of NT-200 carries 24 OM's.

The time calibration is performed with the help of a nitrogen laser positioned just above the array.[11] The 1-ns light flashes of the laser are transmitted by optical fibers of equal length to each of the OM pairs.

3. Laser Experiments

For the two experiments described in this paper an additional laser device was operated at various locations with respect to the PMT's of the neutrino telescope. Short light pulses were emitted by the laser, traveled through the water, and were detected by the PMT's during normal operation, when the standard trigger on the muons crossing the array (three fold coincidence within 500 ns) was set.

The laser module[11] contains a pulsed nitrogen laser (wavelength, 337.1 nm) that pumps a dye laser with an emission maximum at 475 nm. This wavelength is a good match with the point of maximum transparency at 490 nm, where Baikal water has an absorption length of ~20 m.

The light pulses generated by the laser have a length of ~0.5 ns (FWHM), thus being shorter than the time resolution of the photomultipliers. An attenuation disk moved by a stepper motor is used to attenuate the light beam in five steps from 100% to 0.3% of the laser intensity of $\sim 10^{12}$ photons/pulse. Both lasers, the attenuator, power supplies, and a microcomputer are contained in a glass pressure vessel of 155-mm diameter and 1-m length (see Fig. 3). After having crossed the vessel wall, the laser beam is directed into a hollow sphere with a diffusely reflecting inner surface (isotropizer). Through small holes in the sphere the light is able to escape with a nearly isotropic distribution. Owing to the large distance to the detector, the laser module can be considered an isotropic pointlike light source.

The laser can be triggered to generate cycles of light pulses. Each cycle consists of five series of 200 equally intense pulses. The intensities of consecutive series differ by a factor of 3–4. Laser-induced events fulfill the trigger conditions for muons crossing the array. They can be separated from those using the periodicity of the laser pulses (9.1 Hz). The remaining background from muon events ranges from 10^{-3} for low light intensities to 10^{-4} for higher intensities.

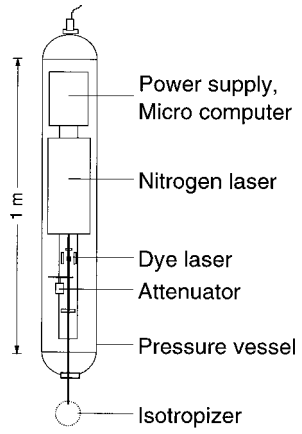

Fig. 3. Schematic view of the laser module.

In the following, data taken with two configurations are analyzed:

1995 Experiment. In April 1995 an intermediate version of the final array, NT-200, was deployed. It carried 72 optical modules mounted at four short strings and one long string (see Fig. 4). The laser experiment was performed immediately after deployment of this detector (NT-72). The laser module was deployed from the ice surface and placed at several locations 20–200 m from the PMT's. Preliminary results from this experiment have been published in Refs. 12 and 13.

1997 Experiment. The 1997 laser experiment was performed after having deployed the first string of the 1997 season. The string carried 24 PMT's with the highest at a 1059-m depth and the lowest at a 1128-m depth. The laser was moved along the string at a horizontal distance of 12 m to the string with the PMT's, starting at a height close to the top

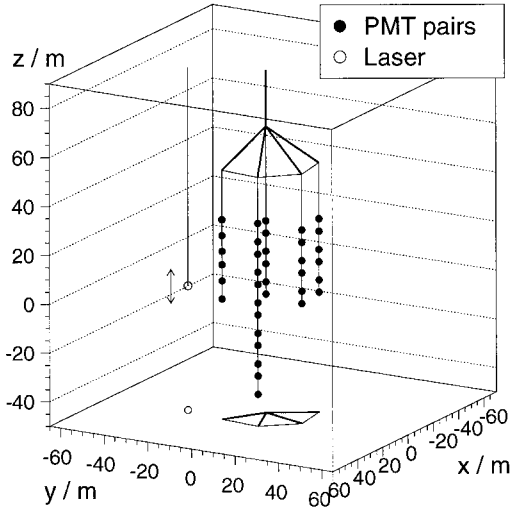

Fig. 4. Schematic view of the 1995 configuration of the laser experiment. Each filled circle represents a pair of OM's (channel). The laser is indicated by the open circle.

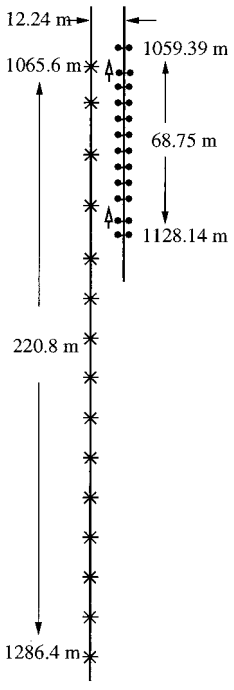

Fig. 5. Schematic view of the 1997 configuration of the laser experiment. Channels are shown explicitly as pairs of OM's. The various positions of the laser are indicated by asterisks. The OM's face down with the exception of channels 2 and 11 (upward arrows) that are directed upward.

PMT. The last of the 15 positions was 221 m below the first, at 1286 m (see Fig. 5).

In both experiments the times and amplitudes of the fired channels were recorded if the standard trigger on the muons crossing the array (three fold coincidence within 500 ns) was fulfilled.

4. Light Field of an Isotropic Source in a Medium

The photon field $\Phi(R, \mathbf{\Omega}, t)$ produced in a medium by a pulsed pointlike source of monochromatic light is a function of distance R from the light source, direction vector $\mathbf{\Omega}$, and time t after emission. This function can be calculated by Monte Carlo methods with λ_{abs}, λ_{sct}, and $\beta(\theta)$ as input parameters. In this section we derive analytical approximations for the photon field and compare it with results of Monte Carlo simulations.

In the special case of a medium without scattering one has

$$\Phi(R, \mathbf{\Omega}, t) = F(R)\delta(\mathbf{\Omega})\delta(t - R/v), \tag{1}$$

where $F(R)$ is the photon flux:

$$F(R) = \int \Phi(R, \mathbf{\Omega}, t)\mathrm{d}\mathbf{\Omega}\mathrm{d}t = \frac{I_0}{4\pi R^2}\exp\left(-\frac{R}{\lambda_{abs}}\right). \tag{2}$$

For a medium with scattering, $F(R)$ can be written as

$$F(R) = \frac{I_0}{4\pi R^2}\exp\left[-\frac{R}{\lambda_{abs}}\mu(R)\right], \tag{3}$$

where in the general case $\mu(R)$ is some intricate function of R. This function takes into account the increase in the photon path that is due to scattering. It was shown in Ref. 14 that $1 < \mu(R) < 1.01$ for distances $R < 0.6\lambda_{sct}$ and steep scattering functions ($\langle\cos\theta\rangle \geq 0.9$). At greater distances, however, the contribution from scattering becomes significant. In the following we estimate the influence of scattering on the photon flux at moderate distances from the source.

Owing to scattering, a photon does not travel along a straight line but follows some polygonal path with random vectors $\mathbf{r}_i (i = 1, 2, \ldots, n)$, which are the trajectories of a photon between two successive scattering acts. Thus

$$\langle r_i\rangle = \lambda_{sct}, \tag{4}$$

$$\langle\mathbf{r}_i \cdot \mathbf{r}_{i+1}\rangle = \lambda_{sct}{}^2\langle\cos\theta\rangle. \tag{5}$$

The result is that, under somewhat general assumptions about the shape of the scattering function, the following relation takes place:

$$\langle\cos\theta_{i,\,i+k}\rangle = \langle\cos\theta\rangle^k, \tag{6}$$

where $\theta_{i,\,i+k}$ is the angle between vectors $\mathbf{r}_i$ and $\mathbf{r}_{i+k}$. In this case

$$R = \left(\sum_{i=1}^{n}\sum_{j=1}^{n}\langle\mathbf{r}_i \cdot \mathbf{r}_j\rangle\right)^{1/2} = \lambda_{sct}\left[n + 2\sum_{i=1}^{n}(n-k)\langle\cos\theta\rangle^k\right]^{1/2}. \tag{7}$$

The average length L of the photon path for n successive scattering acts is

$$L = n\lambda_{sct}. \tag{8}$$

For simplicity we consider the case of $\langle\cos\theta\rangle$ close to 1. With $(1 - \langle\cos\theta\rangle)$ being small, from Eqs. (7) and (8) one gets

$$L(R) \approx R\left[1 + \frac{1}{3}\frac{R}{3\lambda_{sct}}(1 - \langle\cos\theta\rangle)\right]^{1/2}. \tag{9}$$

For water with strongly forward peaked scattering we finally obtain

$$F(R) = \frac{I_0}{4\pi R^2}\exp\left\{-\frac{R}{\lambda_{abs}}\left[1 + \frac{1}{3}\frac{R}{\lambda_{sct}}(1 - \langle\cos\theta\rangle)\right]^{1/2}\right\}. \tag{10}$$

We note that in Eq. (10) λ_{sct} and $\langle\cos\theta\rangle$ are combined in an expression $\lambda_{sct}/(1 - \langle\cos\theta\rangle)$, resulting in a reduction in the number of independent parameters in Eq. (10) from three to two. This agrees with conclusions in Ref. 15 from the measurements of the photon flux of an isotropic source in artificial media as well as in natural water. For all these strongly forward-scattering media it was found that $F(R)$ can be de-

scribed as a function of only two parameters, λ_{abs} and P, where

$$P = \frac{\lambda_{abs}}{\lambda_{sct}} \frac{\langle \theta^2 \rangle}{2}. \quad (11)$$

Since for $\langle \cos\theta \rangle \simeq 1$ one has $\langle \theta^2 \rangle \approx 2(1 - \langle \cos\theta \rangle)$, Eq. (10) can be rewritten in terms of parameters λ_{abs} and P:

$$F(R) = \frac{I_0}{4\pi R^2} \exp\left[-\frac{R}{\lambda_{abs}} \left(1 + \frac{1}{3} \frac{R}{\lambda_{abs}} P \right)^{1/2} \right]. \quad (12)$$

Our Monte Carlo simulations[16] confirm the results of Ref. 15, which proved that, for an interval $\langle \theta^2 \rangle = 0.114-0.582$ and for distances $R < 5\lambda_{abs}$, the error in $F(R)$ resulting from the reduction of λ_{scat} and $\beta(\theta)$ to P is less than 1%.

With the notation

$$\lambda_{eff} = \frac{\lambda_{sct}}{1 - \langle \cos\theta \rangle}, \quad (13)$$

Eq. (10) can be rewritten as

$$F(R) = \frac{I_0}{4\pi R^2} \exp\left[-\frac{R}{\lambda_{abs}} \left(1 + \frac{1}{3} \frac{R}{\lambda_{eff}} \right)^{1/2} \right]. \quad (14)$$

The definition of λ_{eff} according to Eq. (13) coincides with the one for the diffusion case provided $\langle \cos\theta \rangle$ is close to zero (i.e., quasi-isotropic scattering), and in the expansion in powers of $\langle \cos\theta \rangle$ only the first correction term is taken into account. We emphasize that in our case λ_{eff} is just a convenient, artificial parameter [comparable, e.g., to parameter P in Eq. (12)] and should not be associated with an effective increase in the scattering length owing to the anisotropy of the scattering.

Although Eq. (14) was derived here for strongly forward peaked scattering functions, similar considerations can also be performed for the case in which $\langle \cos\theta \rangle$ is not close to unity as, for example, in glacier ice, which is exploited for the AMANDA neutrino telescope.[17]

Equation (12) may also be considered as a particular solution of the transport equation for the small-angle approximation. Within the framework of the small-angle approximation the general solution has the form (see, e.g., Ref. 18)

$$F(R) = \frac{I_0}{4\pi R^2} \frac{(R\sqrt{P}/\lambda_{abs})}{\sinh(R\sqrt{P}/\lambda_{abs})} \exp\left(-\frac{R}{\lambda_{abs}} \right). \quad (15)$$

Equation (12) can be formally found from the solution [Eq. (15)] by expansion with respect to the small parameter, $R\sqrt{P}/\lambda_{abs}$. The opposite case, $R\sqrt{P}/\lambda_{abs} \gg 1$, gives

$$F(R) = \frac{I_0 \sqrt{P}}{2\pi R \lambda_{abs}} \exp\left[-\frac{R}{\lambda_{abs}} (1 + \sqrt{P}) \right]$$

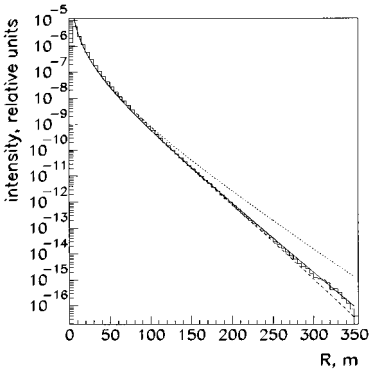

Fig. 6. Intensity versus distance as obtained from Monte Carlo calculations (histogram), Eq. (12) (dashed curve), and Eq. (15) (solid curve). In all three cases $\lambda_{abs} = 23$ m and $P = 0.1$ have been used. The dotted curve is the result of Eq. (3) with $\mu(R) = 1$.

$$= \frac{I_0}{2\pi R(\lambda_{abs}\lambda_{eff})^{1/2}} \exp\left\{ -\frac{R}{\lambda_{abs}} [1 + (\lambda_{abs}/\lambda_{eff})^{1/2}] \right\}. \quad (16)$$

In Fig. 6 we compare the results of our Monte Carlo simulations (histogram) with the predictions of Eq. (12) (dashed curve) and Eq. (15) (solid curve) for $\lambda_{abs} = 23$ m and $P = 0.1$. The dotted curve represents the result of Eq. (3) with $\mu(R) = 1$ (the case without scattering). One observes the perfect agreement of Eq. (15) with the Monte Carlo calculations over a wide region of distances. For not too large distances Eq. (12) also agrees with the Monte Carlo data.

In Section 5 we apply the expressions obtained to the experimental data.

5. Analysis of Experimental Data

A. Absorption

1. 1995 Experiment

The absorption of light on its way to the photomultipliers can be determined from the measured amplitudes. For the 1995 laser experiment, 24 of the 72/2 = 36 channels have been included in the analysis. The combination of amplitudes from different photomultipliers requires careful calibration. After amplitude calibration and by using the well-known angular acceptance of the photomultipliers, we converted the mean amplitudes measured by each channel of NT-72 to light intensities. Figure 7 shows the dependence of photon density on the laser distance. The points represent the measured signals from the optical modules that face the laser for different laser positions and intensities.

The data are well described by

$$F(R) \sim \frac{1}{R^2} \exp\left(-\frac{R}{\lambda} \right) \quad (17)$$

over a wide region of distances R. This is the approximation of Eq. (14) for the $R/(3\lambda_{eff}) \ll 1$ case.

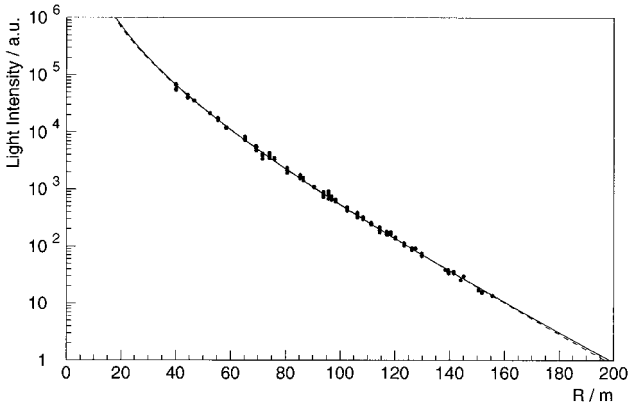

Fig. 7. Laser experiment 1995: light intensity as a function of the distance to the laser. The dots show the measured values, the solid curve shows an exponential decrease with $\lambda = 19.9$ m. If scattering is included, the dependence shown by the dashed curve is expected.

With $\lambda_{\text{eff}} \approx 400$–$500$ m (see Subsection 5.B) and R covering the 30–150-m range, the latter condition is satisfied. Therefore λ in Eq. (17) can be identified with the absorption length λ_{abs}. The value of λ_{abs} obtained from the experimental data of 1995 is (19.9 ± 0.2) m.[12]

2. 1997 Experiment

In Fig. 8 we present the average amplitudes multiplied with R^2 versus distances R for one of the channels of the first 1997 telescope string. The data points can be grouped along five straight lines, each corresponding to a given intensity of the laser. Contrary to the experiment of 1995, the analysis was performed for each channel separately. This procedure avoids biases from possible errors in the relative amplitude calibration of the PMT's. The large number of channels (i.e., the multiple independent determination of λ_{abs}) and the high precision of the

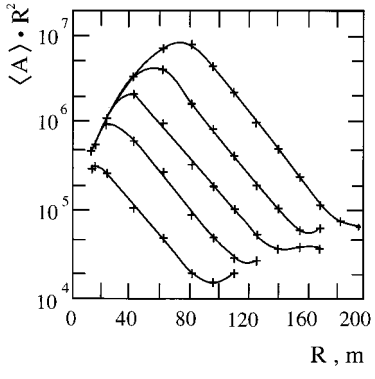

Fig. 8. Laser experiment 1997: logarithm of average amplitude $\langle A \rangle$ times squared distance R^2 versus distance R for one of the 12 channels of the first string. Curves are to guide the eye. Each curve corresponds to one of five different laser intensities. Saturation of the curves at low R is due to the limited dynamic range; flattening at high R is due to the noise. Fits have been applied to the linear part of the curves.

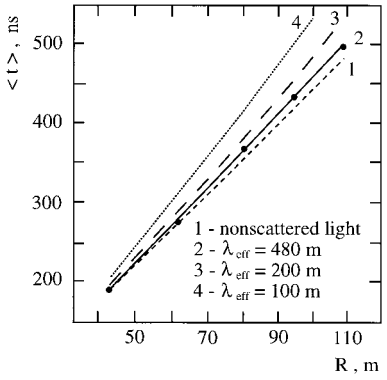

Fig. 9. Laser experiment 1997: average arrival times $\langle t \rangle$ versus distance R. Dots represent the measured values, lines give expectations for different values of the effective scattering length λ_{eff}. In both cases absorption effects have been subtracted (see text).

measured amplitudes and distances result in small errors of λ_{abs}. The absorption length is $\lambda_{\text{abs}} = 22$ m, with variations of ~6%, dependent on the covered range in R. Most of this variation (~5%) is due to the change in λ_{abs} with depth. The errors in the measurement itself are estimated to be smaller than 1% (i.e., 0.2 m). We attribute the discrepancy between the 1995 and the 1997 results to time variations of the water parameters.

B. Scattering

To investigate scattering we evaluated the delay in the arrival times of the photons. According to Eqs. (9) and (13), these times can be written as

$$t = \frac{R}{c_w}\left(1 + \frac{1}{3}\frac{R}{\lambda_{\text{eff}}}\right)^{1/2} \approx \frac{1}{c_w}\left(R + \frac{1}{6}\frac{R^2}{\lambda_{\text{eff}}}\right), \qquad (18)$$

where c_w is the velocity of light in water. Note that this approximation applies only for multiple scattering under small angles. Strongly scattered photons (e.g., caused by Rayleigh scattering) arrive much later and would not coincide with one of the many forward-scattered photons. This, however, is a condition for a channel to trigger because its two OM's coincide. Equation (18) does not include the effects of absorption. Consequently in reality the average time delay is smaller than that given by Eq. (18): Photons traveling a longer path are absorbed and contribute less to the average delay. Absorption is described by the exponential probability distribution of Eq. (14).

With λ_{abs} determined from the intensity-versus-distance curve, the effect of absorption can be subtracted from the experimental data as well as from Monte Carlo data. In Fig. 9 we compare the experimental delays with the delay curves expected from different assumptions on λ_{eff}. For both experiment and prediction the effect of absorption is subtracted so that Eq. (18) can be applied. The solid line gives the best fit and corresponds to $\lambda_{\text{eff}} = 480$ m. The error of λ_{eff} is estimated as 15%.

The value of λ_{eff} obtained in the present work can

be compared with the results of the direct measurements of λ_{sct} and $\beta(\theta)$ cited in Refs. 2 and 7. There, with the help of the measured scattering function $\beta(\theta)$, $\langle\cos(\theta)\rangle \approx 0.95$–$0.96$ was found. For λ_{sct}, values of 15–18 m were obtained. In 1997 (not published) we measured $\langle\cos(\theta)\rangle \approx 0.9$ and $\lambda_{sct} = 40$–50 m. With Eq. (13) this results in $\lambda_{eff} = 300$–450 m and $\lambda_{eff} = 400$–500 m (1997), compatible with $\lambda_{eff} = 480 \pm 70$ m determined in the present analysis. We note that for $\langle\cos(\theta)\rangle$ close to 1 the result is extremely sensitive to the exact value of $\langle\cos(\theta)\rangle$. Also, scattering parameters in Lake Baikal are known to vary strongly with time. This makes the agreement even more satisfactory.

C. Asymptotic Attenuation Length

As follows from Eq. (16), at large distances

$$F(R) \sim \frac{1}{R}\exp\left(-\frac{R}{\lambda_{asm}}\right), \tag{19}$$

where

$$\lambda_{asm} = \frac{\lambda_{abs}}{1 + (\lambda_{abs}/\lambda_{eff})^{1/2}} \tag{20}$$

is the so-called asymptotic attenuation length. Equation (16) describes the asymptotic behavior of $F(R)$. In the asymptotic regime, angular and spatial dependences of $\Phi(R, \mathbf{\Omega}, t)$ can be factored (see, for example, Refs. 19 and 20) so that

$$\int \Phi(R, \mathbf{\Omega}, t)\mathrm{d}t = F(R)\rho(\mathbf{\Omega}). \tag{21}$$

Therefore the measurement of λ_{asm} is not sensitive to the orientation of the PMT's and can be performed independently for various directions.

Although Eq. (16) follows from Eq. (15) only for large distances, our Monte Carlo simulations show that the $\exp[-(R/\lambda_{asm})]/R$ behavior is already seen for $R \approx 100$ m if $\lambda_{abs} \approx 20$ m, $\lambda_{eff} \leq 500$ m, and the channel faces away from the light source. Photons observed by these channels are scattered very often and form a light field close to the asymptotic propagation regime. Thus the value of λ_{asm} can be evaluated from the data of the 1997 laser experiment where the maximal distance R was ~180 m. Figure 10 shows the R dependence of the amplitudes for channel 2, looking away from the source. The experimental data behave exponentially with an exponent $1/L_{\uparrow} \approx 1/(17.6 \pm 0.5)m^{-1}$.

Comparing Monte Carlo simulations with Eq. (15), we found that in the general case $0.95L_{\uparrow} \leq \lambda_{asm} \leq 1.05L_{\uparrow}$, and so we finally obtain $\lambda_{asm} = (17.6 \pm 1.5)$ m.

Since there is a certain overlap between the regions in which both approximation (19) and Eq. (14) describe the photon flux as a function of distance, one could try to estimate λ_{eff} from λ_{asm} and λ_{abs}, by using Eq. (20). Unfortunately, the final result is sensitive to the exact values of asymptotic and absorption length [compare what was said above about the estimation of λ_{eff} from $\langle\cos(\theta)\rangle$]. Therefore the available accuracy of our experiments does not yet allow a determination of λ_{eff} in this way. However, λ_{asm} itself can be applied as a useful parameter for the description of the photon flux at large distances.

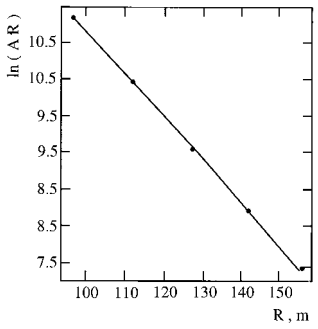

Fig. 10. Logarithm of the product of average amplitude $\langle A\rangle$ and R versus distance R in the asymptotic regime for channel 2, looking away from the laser.

6. Conclusions

We have used a neutrino telescope triggered by laser light pulses to measure the optical properties of clear, open water with high accuracy. For 1-km-deep water in Lake Baikal in 1997 we determined an absorption length of 22.0 ± 1.2 m and an asymptotic attenuation length of 17.6 ± 1.5 m. Quite different from standard methods, the effective scattering length was obtained from nanosecond timing measurements. It was measured as 480 ± 70 m, which under the assumption of $\langle\cos\theta\rangle = 0.95$ (0.9) translates to a geometric scattering length of 24 (48) m.

In the future we want to refine these measurements by using a larger number of optical modules and measuring over an extended range of distances between optical modules and the laser. Also, we plan a continuous monitoring of the optical parameters over a full year.

Appendix A: Authors' Affiliations

L. Bezrukov, I. Danilchenko, Z-A. Dzhilkibaev, G. Domogatsky, A. Doroshenko, O. Gaponenko, A. Garus, A. Klabukov, S. Klimushin, A. Koshechkin, B. Lubsandorzhiev, A. Panfilov, D. Petukhov, P. Pokhil, and I. Sokalski are with the Institute for Nuclear Research, Russian Academy of Sciences, 60-th October Anniversary Prospect 7a, 117312 Moscow, Russia. V. Balkanov, A. Chensky, N. Budnev, T. Gress, S. Lovzov, R. Mirgazov, A. Moroz, S. Nikiforov, Y. Parfenov, A. Pavlov, P. Pokolev, V. Rubzov, and B. Tarashansky are with the Physical Department, Irkutsk State University, 20 Blvd. Gagarin, 664003 Irkutsk, Russia. L. Kuzmichev, N. Moseiko, E. Osipova, E. Popova, and I. Yashin are with the Institute for Nuclear Research, Moscow State University, Vorobjevy Gori, 119899 Moscow, Russia. S. Fialkovsky, V. Kulepov, and M. Milenin are with the Nizhni Novgorod State Technical University, Minina

4, 603600 Nizhni Novgorod, Russia. M. Rozanov is with the St. Petersburg State Marine Technical University, Locmanskaja 3, 190008 St. Petersburg, Russia. A. Klimov is with the Kurchatov Institute, Kurchatov square 1, 123182 Moscow, Russia. I. Belolaptikov is with the Joint Institute for Nuclear Research, 141980 Dubna, Russia. When this research was performed, A. Karle, T. Mikolajski, D. Pandel, C. Spiering, O. Streicher, and R. Wischnewski were with the Deutsches Elektronen-Synchrotron DESY Zeuthen, Platanenallee 6, D-15738 Zeuthen, Germany. A. Karle is now with the Department of Physics, University of Wisconsin, 1150 University Avenue, Madison, Wisconsin 53706. D. Pandel is now with the Department of Physics, University of California Irvine, Irvine, California 92697. The e-mail address for C. Spiering is csspier@ifh.de.

This work was supported by the Russian Foundation for Basic Research grant 97-05-96466.

References

1. L. B. Bezrukov, N. M. Budnev, Zh. A. M. Dzhilkibaev, M. D. Galperin, O. Yu. Lanin, and B. A. Tarashchanskii, "Measurement of the light absorption coefficient in Lake Baikal water," Oceanology **30,** 1022–1026 (1990), in Russian.
2. O. N. Gaponenko, R. R. Mirgazov, and B. A. Tarashchanskii, "Reconstruction of the primary hydrooptical characteristics from the light field of a point source," Atmos. Oceanic Opt. **9,** 677–682 (1996).
3. H. Bradner and G. Blackinton, "Long baseline measurements of light transmission in clear water," Appl. Opt. **23,** 1009–1012 (1984).
4. R. A. Maffione, K. J. Voss, and R. C. Honey, "Measurement of the spectral absorption coefficient in the ocean with an isotropic source," Appl. Opt. **32,** 3273–3279 (1993).
5. E. G. Anassontzis, P. Ioannou, Chr. Kourkoumelis, L. K. Resvanis, and H. Bradner, "Light transmissivity in the NESTOR site," Nucl. Instrum. Methods A **349,** 242–246 (1994).
6. N. G. Jerlov, *Marine Optics*, Vol. 5 of the Elsevier Oceanography Series (Elsevier, New York, 1976).
7. B. A. Tarashchanskii, O. N. Gaponenko, and V. I. Dobrynin, "On a technique for measuring the scattering phase function using the light field from a source with a wide directional pattern," Atmos. Oceanic Opt. **7,** 819–823 (1994).
8. B. A. Tarashchanskii, R. R. Mirgazov, and K. A. Pochejkin, "Stationary deep-water meter of hydrooptical parameters," Atmos. Oceanic Opt. **8,** 771–774 (1995).
9. S. Barwick, "High energy neutrino observatories: status and future," Nucl. Phys. B (Proc. Suppl.) **43,** 183–193 (1995).
10. Baikal Neutrino Collaboration, "The Baikal underwater neutrino telescope: design, performance, and first results," Astropart. Phys. **7,** 263–282 (1997).
11. Th. Mikolajski, "Methodische Untersuchungen und Kalibration des Baikal Neutrino Teleskops," Ph.D. dissertation (Humboldt-Universität Berlin, DESY-Zeuthen 95-03, 1995), http://www.ifh.de/nuastro/publications/.
12. Baikal Neutrino Collaboration, "Response of the NT-36 array to a distant pointlike light source," *Proceedings of the 24th International Cosmic Ray Conference* (Instituto Nazionale Fisica Nucleare (INFN), Rome, 1995), Vol. 1, pp. 1043–1046.
13. D. Pandel, "Bestimmung von Wasser- und Detektorparametern und Rekonstruktion von Myonen bis 100 TeV mit dem Baikal-Neutrinoteleskop NT-72," Diploma thesis (Humboldt-Universität Berlin, DESY-Zeuthen, 1996), http://www.ifh.de/nuastro/publications/.
14. D. Bauer, J. C. Brun-Cottan, and A. Saliot, "Princip d'une measure directe dans l'eau de mer du coefficient d'absorption de la lumiere," Cah. Oceanogr. **23,** 841–850 (1971).
15. V. N. Pelewin and T. M. Prokudina, "Determination of the absorption coefficient of sea water by the parameters of an isotropic source," *Atmospheric and Oceanic Optics* (Nauka, Moscow, 1972), pp. 148–157 in Russian.
16. O. Ju. Lanin, "Determination of optical parameters of medium with strong anisotropic scattering function," Diploma thesis (Moscow Engineering Physical Institute, Moscow, 1989).
17. P. Askebjer, S. W. Barwick, L. Bergstrom, A. Bouchta, S. Carius, A. Coulthard, K. Engel, B. Erlandsson, A. Goobar, L. Gray, A. Hallgren, F. Halzen, P. O. Hulth, J. Jacobsen, S. Johansson, V. Kandhadai, I. Liubarsky, D. Lowder, T. Miller, P. C. Mock, R. Morse, R. Porrata, P. B. Price, A. Richards, H. Rubinstein, E. Schneider, Q. Sun, S. Tilav, C. Walck, and G. Yodh, "Optical properties of the South Pole ice at depths between 0.8 and 1 kilometer," Science **267,** 1147–1150 (1995).
18. A. S. Monin, *Oceanic Optics, Vol. 1* (Nauka, Moscow, 1983).
19. L. S. Dolin, "On a technique for calculation of the brightness at large optical distances from a light source," Bull. Acad. Sci. USSR Atmos. Oceanic Phys. **17,** No. 1, 102–109 (1981) (in Russian).
20. R. A. Maffione and J. S. Jaffe, "The average cosine due to an isotropic light source in the ocean," J. Geophys. Res. **100,** 13,179–13,192 (1995).